Expression and Targeting of CX_3CL1 (Fractalkine) in Renal Tubular Epithelial Cells

Anne M. Durkan,*† R. Todd Alexander,*† Guang-Ying Liu,† Min Rui,† Giuseppe Femia,† and Lisa A. Robinson*†

*Division of Nephrology and †Research Institute, Hospital for Sick Children, Toronto, Ontario, Canada

The chemokine CX_3CL1 plays a key role in glomerulonephritis and can act as both chemoattractant and adhesion molecule. CX_3CL1 also is upregulated in tubulointerstitial injury, but little is known about the subcellular distribution and function of CX_3CL1 in renal tubular epithelial cells (RTEC). Unexpectedly, it was found that CX_3CL1 is expressed predominantly on the apical surface of tubular epithelium in human renal transplant biopsy specimens with acute rejection or acute tubular necrosis. For studying the targeting of CX_3CL1 in polarized RTEC, MDCK cells that expressed untagged or green fluorescent protein–tagged CX_3CL1 were generated. The chemokine was present on the apical membrane and in subapical vesicles. Apical targeting of CX_3CL1 was not due to signals that were conferred by its intracellular domain, to associations with lipid rafts, or to O-glycosylation but, rather, depended on N-linked glycosylation of the protein. With the use of fluorescence recovery after photobleaching, it was found that CX_3CL1 is immobile in the apical membrane. However, CX_3CL1 partitioned with the triton-soluble rather than -insoluble cellular fraction, indicating that it is not associated directly with the actin cytoskeleton or with lipid rafts. Accordingly, disruption of rafts through cholesterol depletion did not render CX_3CL1 mobile. For exploration of potential functions of apical CX_3CL1, binding of CX_3CR1-expressing leukocytes to polarized RTEC was examined. Leukocyte adhesion to the luminal surface was enhanced significantly when CX_3CL1 was present. These data demonstrate that CX_3CL1 is expressed preferentially on the apical membrane of RTEC and suggest a novel function for the chemokine in recruitment and retention of leukocytes in tubulointerstitial inflammation.

J Am Soc Nephrol 18: 74–83, 2007. doi: 10.1681/ASN.2006080862

Renal tubulointerstitial inflammation is characterized by recruitment of circulating leukocytes to the site of injury. Traffic signals for leukocyte migration are provided by chemokines, a family of small molecular weight proteins (1). Among the chemokines, CX_3CL1 (fractalkine) has a unique role in the inflammatory cascade because of its structure: an extracellular chemokine domain and mucin stalk, tethered to a transmembrane region and a 37–amino acid cytoplasmic tail. Transmembrane CX_3CL1 is cleaved proximal to the membrane by metalloproteinases of the A disintegrin and metalloproteinase (ADAM) family to release a soluble species (2–5). Soluble CX_3CL1 acts as a chemoattractant, whereas the transmembrane protein acts as a cell adhesion molecule for monocytes, natural killer (NK) cells, and subsets of $CD8^+$ T cells, all of which express CX_3CR1, the receptor for CX_3CL1. In this way, CX_3CL1 and CX_3CR1 promote leukocyte infiltration at sites of injury (2,6,7). *In vivo*, CX_3CL1 is strongly implicated in inflammation, including allograft rejection and, most notably, atherogenesis (8–13).

Numerous organs express CX_3CL1, including brain, lung, heart, intestine, and kidney (10,14–17). In humans and rodents, CX_3CL1 expression is prominent in renal glomerular disease, particularly in endothelial and mesangial cells (18–20). The role of CX_3CL1 in mediating glomerular injury is well described in animal models of systemic lupus erythematosus nephritis, mesangioproliferative glomerulonephritis, and crescentic glomerulonephritis (21–23). In these disease processes, blockade of either CX_3CL1 or CX_3CR1 prevents renal injury and leukocyte infiltration (21–23). Little is known, however, regarding the role of CX_3CL1 in tubulointerstitial renal disease. Expression of CX_3CL1 clearly is enhanced in tubulointerstitial injury, including that associated with tubular protein overload and acute allograft rejection (19,24,25). However, knowledge regarding the subcellular distribution and function of CX_3CL1 in renal tubular epithelial cells (RTEC) is rudimentary.

We demonstrate here that CX_3CL1 is present on the apical membrane of RTEC, where it is anchored firmly. We further demonstrate that CX_3CL1 is targeted to the apical membrane *via* N-glycosylation of the chemokine. The implications of apical targeting of CX_3CL1 for the pathogenesis of tubulointerstitial inflammation are discussed.

Materials and Methods

Cells and Constructs

HK-2 cells were a gift from Dr. Andras Kapus, (University of Toronto, Toronto, ON, Canada). MDCK cells were from American Type Culture Collection (Manassas, VA). MDCK cells that stably expressed sodium-hydrogen exchanger 3 (NHE3) tagged with hemagglutinin (HA) were provided by Dr. Sergio Grinstein (University of Toronto).

Received August 15, 2006. Accepted October 19, 2006.

Published online ahead of print. Publication date available at www.jasn.org.

Address correspondence to: Dr. Lisa A. Robinson, Division of Nephrology, Hospital for Sick Children, 555 University Avenue, Toronto, ON, Canada. Phone: 416-813-7654 ext. 1745; Fax: 416-813-6271; E-mail: lisa.robinson@sickkids.ca

ISSN: 1046-6673/1801-0074

The preceding cells were cultured in DMEM and Ham's F12 (Wisent, St-Bruno, Quebec, Canada) that contained 5% FCS. K562 erythroleukemia cells and K562 cells that stably expressed CX_3CR1 (K562-CX_3CR1) were from Dr. Dhavalkumar Patel (University of North Carolina, Chapel Hill, NC) and were cultured in RPMI supplemented with HEPES and 15% FCS. Primary human RTEC (Clonetics, Cambrex, Walkersville, MD) were a gift from Dr. Jim Scholey (University of Toronto) and were cultured according to the manufacturer's instructions (26). CX_3CL1 expression in these cells was verified by Western blotting (27). Human peripheral blood mononuclear cells (PBMC) were isolated from heparinized peripheral blood from healthy volunteers (28).

DNA constructs for CX_3CL1 or CX_3CL1 tagged with green fluorescent protein (CX_3CL1-GFP) were created as described previously (6,27,29). MDCK cells were stably transfected with these constructs using FuGENE (Roche, Indianapolis, IN) and selected in 500 μg/ml G418 (Wisent).

The predicted transmembrane portion of CX_3CL1 ends at amino acid 360 (PSORT II). A mutant construct that lacked amino acids 361 to 397, CX_3CL1–360, was generated by PCR using the common upstream primer 5′-GTGGAATTCTGCAGTCGACTC-3′ and the downstream primer 5′-GCGGCCGCTCACATGGCCACCCCCAGGCAG-3′. In the downstream primer, stop codons and NotI sites were introduced. PCR products were cloned into TOPO vector (Invitrogen, Burlington, ON, Canada) and sequenced. Inserts were released by cutting with NotI and EcoRI and subcloned into HA-pcDNA3.1 (Invitrogen). MDCK cells were transfected using FuGENE and selected in 500 μg/ml G418 (MDCK-CX_3CL1–360). DNA constructs that encoded GFP-tagged glycosyl phosphatidylinositol (GPI-GFP) and FcRIIa receptor (FcR-GFP) were a gift from Dr. S. Grinstein (University of Toronto) (30,31).

Antibodies and Reagents

The following antibodies were used: Goat anti-human CX_3CL1 directed against the extracellular chemokine region (R&D Systems, Minneapolis, MN) (19,32), goat anti-human CX_3CL1 against the intracellular carboxy terminus (Santa Cruz Biotechnology, Santa Cruz, CA), anti-actin (Sressgen, Victoria, BC, Canada), and anti-HA (Covance, Berkeley, CA). Cy3- and horseradish peroxidase–conjugated anti-goat IgG, anti-mouse IgG, and 18 nm gold-labeled anti-goat IgG were from Jackson Immunoresearch Laboratories (Bar Harbor, ME). Tunicamycin, benzyl-2-acetamido-2-deoxy-α-D-galacto-pyranoside, and methyl-β-cyclodextrin (MβCD) were from Sigma-Aldrich (St. Louis, MO). Amplex Red kit was used to measure cholesterol levels (Molecular Probes, Eugene, OR). Cholera toxin B conjugated to Alexa fluor 555 was from Molecular Probes. The metalloprotease inhibitors TAPI-2 and GM6001 were from Peptides International (Louisville, KY) and Chemicon International (Temecula, CA), respectively. TNF-α was from R&D Systems.

Immunohistochemistry

Renal transplant biopsy specimens were obtained in accordance with the guidelines of the Research Ethics Board of University Health Network (University of Toronto). Frozen 7-μM sections were air-dried and fixed in acetone. After blocking with 5% donkey serum, sections were incubated with anti-CX_3CL1 antibody (Ab), followed by Cy3-conjugated anti-goat IgG.

Immunofluorescence staining of cultured cells was performed as described previously (33). For detection of surface CX_3CL1, cells were fixed and labeled with anti-CX_3CL1 Ab and Cy3-conjugated secondary Ab. For detection of surface and intracellular CX_3CL1, the same cells were permeabilized with 0.1% Triton X-100 and incubated again with anti-CX_3CL1 Ab and Cy5-conjugated secondary Ab. In some experiments, Alexa 488–conjugated phalloidin was added with the secondary Ab to label F-actin. Cells were visualized using either an LSM 510 confocal microscope (Zeiss, Toronto, ON, Canada) or a spinning disk DMIRE2 confocal microscope (Leica Microsystems, Toronto, ON, Canada), equipped with an Hamamatsu backthinned EM-CCD camera. Images were acquired using 100× oil immersion and the appropriate filters. Z stacks were constructed and images deconvolved using Velocity software (Improvision, Lexington, MA).

PCR

RNA was isolated from HK-2 cells using Trizol (Life Technologies, Burlington, ON, Canada), and reverse transcriptase–PCR for CX_3CL1 was performed using oligo(dT) and specific primers (24). PCR products were size-fractionated on 1% agarose in TBE gels and stained with ethidium bromide.

Immunoblotting

SDS-PAGE and immunoblotting were performed using anti-CX_3CL1 Ab (0.2 μg/ml) (27,34). Immunoreactive bands were visualized by enhanced chemiluminescence (Amersham Biosciences UK Limited, Buckinghamshire, UK) recorded on x-ray film. Detergent resistance was assessed as described previously (34). Triton-soluble and -insoluble components were compared with total cell lysate.

Electron Microscopy

Scanning electron microscopy (EM) was performed as described previously using anti-CX_3CL1 Ab (1 μg/ml) and 18 nm of gold-labeled anti-goat IgG secondary antibody (34).

Fluorescence Recovery after Photobleaching

Experiments were performed as described previously (34,35). Briefly, the apical surface was brought into focus on a confocal microscope, and two 2.5-μm diameter areas of similar fluorescence intensity were selected per cell. After acquisition of baseline measurements, one defined area was photobleached irreversibly, and fluorescence of both areas was measured over time. Fractional fluorescence recovery of the bleached area was determined relative to prebleach measurements. The unbleached area was used to control for inadvertent bleaching during repeated image acquisition. Results are expressed as the mean fluorescence recovery for at least six experiments, with SEM.

Adhesion Assays

Experiments were performed as described elsewhere with minor modifications (10). Briefly, MDCK-CX_3CL1-GFP cells were grown to confluence on 25-mm coverslips and pretreated with 10 μM TAPI-2 for 2 h to maximize cell surface expression of CX_3CL1. K562-CX_3CR1 cells were labeled with cholera toxin B-555, and 1×10^6 cells were added to wells of either MDCK or MDCK-CX_3CL1-GFP cells with gentle rocking at 10 cycles/min. Nonadherent cells were washed away, and remaining cells were fixed and mounted onto slides. Using a Leica deconvolution microscope, we examined at least 50 high-power fields (×63) to count the number of adhered cells. Results are the mean of three separate experiments with SEM and were compared using paired *t* test. Cells also were examined using a spinning disk confocal microscope.

Results

CX_3CL1 Is Expressed in RTEC

To define the functions of CX_3CL1 in RTEC, we first examined CX_3CL1 expression in five human renal allograft biopsy specimens. Three specimens had histologic diagnosis of acute

rejection and two of acute tubular necrosis. In all five specimens, we detected CX_3CL1 expression in renal tubules, particularly on the apical surface (Figure 1, A and B). In addition to being expressed on tubular epithelium, modest CX_3CL1 expression was noted within the glomeruli and on vascular endothelium (data not shown). This is in keeping with a previously published report (19). To verify the specificity of staining, we omitted primary anti-CX_3CL1 Ab from some experiments. When the secondary Ab alone was used, very little background immunofluorescence was observed (data not shown). At our institution, donor preimplantation renal transplant biopsies are not performed routinely and therefore could not be used as an additional negative control. However, using the same anti-CX_3CL1 Ab as the one used in our study, other investigators previously reported minimal immunohistochemical expression of CX_3CL1 in normal renal biopsy tissue (19,32). We then examined expression and subcellular distribution of CX_3CL1 in HK-2 cells, a human RTEC line. Using reverse transcriptase–PCR, we detected CX_3CL1 mRNA (Figure 1C). To verify CX_3CL1 protein expression, we performed immunofluorescence staining and again found the chemokine predominantly at the apical surface (Figure 1D).

CX_3CL1 Is Expressed in the Apical Membrane of RTEC

Because HK-2 cells, unlike other tubular epithelial lines, grow in flattened monolayers, we adopted another approach,

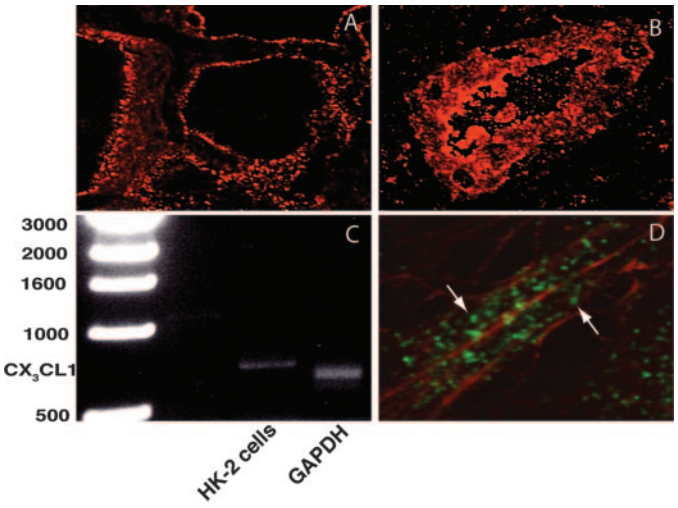

Figure 1. CX_3CL1 is expressed in human renal tubular epithelial cells (RTEC). Immunofluorescent labeling of CX_3CL1 in human renal allograft biopsy specimens, with histologic diagnoses of acute tubular rejection (A) and acute tubular necrosis (B). Samples were labeled with anti-CX_3CL1 antibody (Ab) and Cy3-conjugated secondary Ab. (C) Total RNA was isolated from HK-2 cells, and CX_3CL1 was amplified by reverse transcriptase–PCR using specific published primers. The PCR products were size-fractionated on 1% agarose. Glyceraldehyde-3-phosphate dehydrogenase (GAPDH) is shown as a control. (D) Immunofluorescence staining of HK-2 cells using anti-CX_3CL1 Ab and a Cy2-conjugated secondary Ab. Actin was labeled with rhodamine-conjugated phalloidin. Arrows demonstrate CX_3CL1 labeling on the apical surface of cells.

stably expressing full-length CX_3CL1 or CX_3CL1-GFP in MDCK cells, a renal cell line with cuboidal morphology that is typical of epithelial cells, facilitating distinction between apical and basolateral surfaces. Using Western analysis and anti-CX_3CL1 Ab, MDCK-CX_3CL1 and MDCK-CX_3CL1-GFP cells each displayed a single band of appropriate molecular weight (Figure 2A). For assessment of the subcellular localization of CX_3CL1, MDCK-CX_3CL1-GFP cells (Figure 2B) were fixed and incubated with anti-CX_3CL1 Ab, which labeled only the apical surface (Figure 2C). For visualization of intracellular CX_3CL1, the same cells then were permeabilized and incubated with anti-CX_3CL1 Ab followed by a different secondary Ab. This confirmed an intracellular pool of CX_3CL1 in subapical vesicles (Figure 2D). To confirm that any labeling of MDCK-CX_3CL1-GFP cells with anti-CX_3CL1 Ab was specific for CX_3CL1, we incubated untransfected MDCK cells with the same Ab. In this instance, no immunofluorescence staining was observed (data not shown). To control further for any background staining of Cy3- or Cy5-conjugated secondary Ab used, we also performed experiments in which the primary Ab was omitted. Once again, incubation with secondary Ab alone yielded no immunofluorescence labeling (data not shown). Collectively, these results demonstrate that CX_3CL1 is expressed on the apical plasma membrane as well as within subapical vesicles.

In MDCK-CX_3CL1-GFP cells, GFP is attached to the cytoplasmic tail of the chemokine. Because the tagged construct was recognized by the Ab directed against the extracellular domain of CX_3CL1, the protein expressed must traverse the apical membrane (Figure 2, B and E). We also noted a second pool of GFP, present in the basolateral membrane (Figure 2B). After permeabilization, the basolateral pool of GFP could be labeled by an anti-CX_3CL1 Ab directed against the intracellular domain of the chemokine (data not shown). We believe that basolateral GFP represents the intracellular portion of CX_3CL1 that remains after the extracellular segment has been proteolytically released. Accordingly, Western analysis of MDCK-CX_3CL1-GFP cells using anti-GFP Ab consistently revealed two separate bands. The molecular masses of these bands correlated with full-length CX_3CL1-GFP fusion protein (Figure 2A) or a fusion protein corresponding to the intracellular region of CX_3CL1 together with GFP (35 kD; data not shown). To ensure that the GFP tag did not alter subcellular traffic of CX_3CL1, we examined MDCK cells that expressed the untagged chemokine and found a similar distribution (Figure 2F).

We used scanning EM to confirm that CX_3CL1 is expressed on the apical membrane of RTEC. As shown in Figure 2G, CX_3CL1 is associated with microvilli on the apical surface.

CX_3CL1 Is Targeted to the Apical Membrane by N-Glycosylation

We next investigated the signals that target CX_3CL1 to the apical membrane. Apical sorting of transmembrane proteins can be determined by signals that are conferred by the cytoplasmic tail of the protein (36,37), by O- or N-glycosylation (38), or by membrane anchoring of the protein through GPI or directly to lipid rafts (39). We examined each of these potential mechanisms.

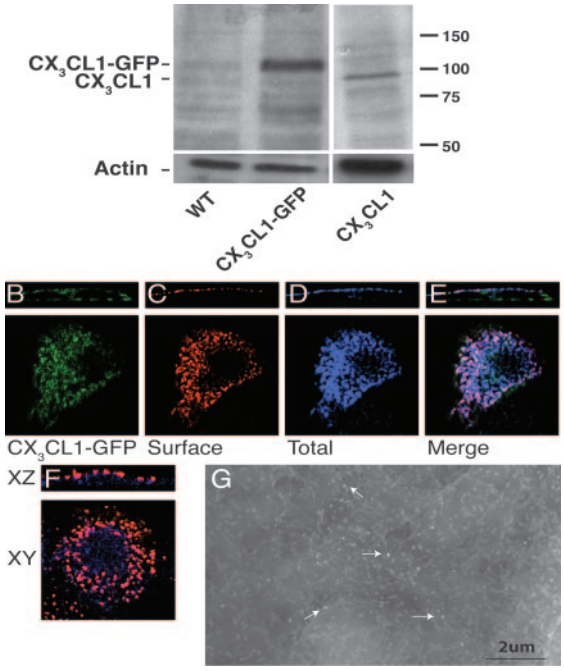

Figure 2. CX_3CL1 is expressed on the apical surface of RTEC. (A) Western analysis was performed using cell lysates from control wild-type MDCK cells (WT), MDCK-CX_3CL1-GFP, and MDCK-CX_3CL1 cells, using anti-CX_3CL1 Ab and horseradish peroxidase (HRP)-conjugated secondary Ab. For MDCK-CX_3CL1-GFP and MDCK-CX_3CL1 cells, bands of predicted molecular weight were obtained, namely 116 and 90 kD, respectively. (B through E) Immunofluorescence labeling of MDCK-CX_3CL1-GFP cells was performed as in Materials and Methods, and cells were examined by spinning disk confocal microscopy. (B) Spinning disk confocal image of MDCK-CX_3CL1-GFP cells. (C) For visualization of CX_3CL1 at the cell surface, MDCK-CX_3CL1-GFP cells were fixed before incubation with anti-CX_3CL1 Ab and Cy3-conjugated anti-goat IgG secondary Ab. (D) For visualization of both surface and intracellular CX_3CL1, cells were fixed and permeabilized before incubation with anti-CX_3CL1 Ab and Cy5-conjugated secondary Ab. (E) Merged images B through D. Images are shown as x *versus* y and x *versus* z optical sections. (F) Examination of the subcellular distribution of untagged CX_3CL1. For visualization of cell surface CX_3CL1, MDCK-CX_3CL1 cells were fixed, then incubated with anti-CX_3CL1 Ab, followed by Cy3-conjugated anti-goat IgG secondary Ab. For visualization of any intracellular CX_3CL1 present, the same cells then were permeabilized and incubated again with anti-CX_3CL1 Ab followed by Cy5-conjugated secondary Ab. (G) MDCK-CX_3CL1-GFP cells were labeled with anti-CX_3CL1 Ab and gold-conjugated secondary Ab and examined using scanning electron microscopy. Arrows show the association of the CX_3CL1 with apical microvilli. Reverse-phase images are shown. Magnification, ×100 in B through E.

To determine whether the cytosolic tail of CX_3CL1 mediates apical targeting, we generated a mutant construct that lacked the cytoplasmic domain (CX_3CL1–360). We examined the distribution of CX_3CL1 in MDCK cells that stably expressed "tailless" CX_3CL1 but found that the protein still was directed to the apical membrane (Figure 3A).

We next assessed potential associations of CX_3CL1 with lipid rafts. We treated cells with MβCD to extract cholesterol, thereby disrupting lipid rafts (40). To ensure that MβCD treatment was effective, we measured cholesterol spectrophotometrically (41). MβCD depleted total cellular cholesterol by 58% ($P < 0.05$; Figure 3B) but had no effect on apical targeting of CX_3CL1 (Figure 3C).

We next examined glycosylation of CX_3CL1 as a determinant of apical targeting. O-glycosylation was inhibited with benzyl-2-acetamido-2-deoxy-α-D-galacto-pyranoside. Again, CX_3CL1 targeting to the apical membrane remained intact (Figure 3D). To inhibit N-glycosylation of CX_3CL1, we treated cells with tunicamycin. This treatment resulted in intracellular retention of CX_3CL1 with virtually no expression observed on the apical surface (Figure 3E). To verify that the observed effects were not due to nonspecific disruption of apical protein traffic, we evaluated the effects of tunicamycin on NHE3, a protein that does not require N-glycosylation for its apical targeting. As expected, tunicamycin treatment did not affect the normal apical distribution of NHE3 (Figure 3F).

Collectively, these data indicate that the signals that direct apical trafficking of CX_3CL1 are not conferred by the protein's cytoplasmic domain, O-glycosylation of the protein, or associations with lipid rafts. Rather, apical localization of CX_3CL1 is determined by N-glycosylation.

CX_3CL1 Is Anchored to the Apical Membrane in RTEC

To determine whether CX_3CL1 is anchored in the luminal surface, we used fluorescence recovery after photobleaching to study the mobility characteristics of apical CX_3CL1-GFP in MDCK-CX_3CL1-GFP cells (see Materials and Methods) (Figure 4, A [before bleaching], B [immediately after bleaching], and C [5 min after bleaching]). As a control, MDCK cells were transfected with a DNA construct that encoded GPI-GFP, which is freely mobile in the apical plasma membrane. A region of the apical membrane was bleached similarly, and the recovery of fluorescence was observed over time (Figure 4, D through F). CX_3CL1-GFP recovered with significantly slower kinetics than GPI-GFP (Figure 4G). For CX_3CL1-GFP, the bleached area recovered to 10.5 ± 4.3% of prebleached fluorescence intensity by 4 min, compared with 61.1 ± 11.9% for GPI-GFP ($P < 0.01$). As an additional control, MDCK cells were transfected with DNA that encoded the single transmembrane protein FcR-GFP. When fluorescence recovery after photobleaching was performed similarly, the bleached area in the membrane recovered significantly faster than CX_3CL1-GFP, with 4-min recovery of 51.5 ± 6.1% for FcR-GFP ($P < 0.01$; Figure 4G). These data demonstrate that the ability of CX_3CL1 to diffuse laterally within the apical membrane is impeded, and, therefore, transmembrane CX_3CL1 is immobile.

Some single-pass transmembrane proteins are tethered to the apical membrane by direct association with lipid rafts (42). To determine whether CX_3CL1 is anchored in such a manner, we disrupted lipid rafts by treating cells with MβCD. However, this treatment did not mobilize CX_3CL1 in the apical membrane (Figure 4G). To study whether apical CX_3CL1 is immobile because it is tethered directly to the actin cytoskeleton, we

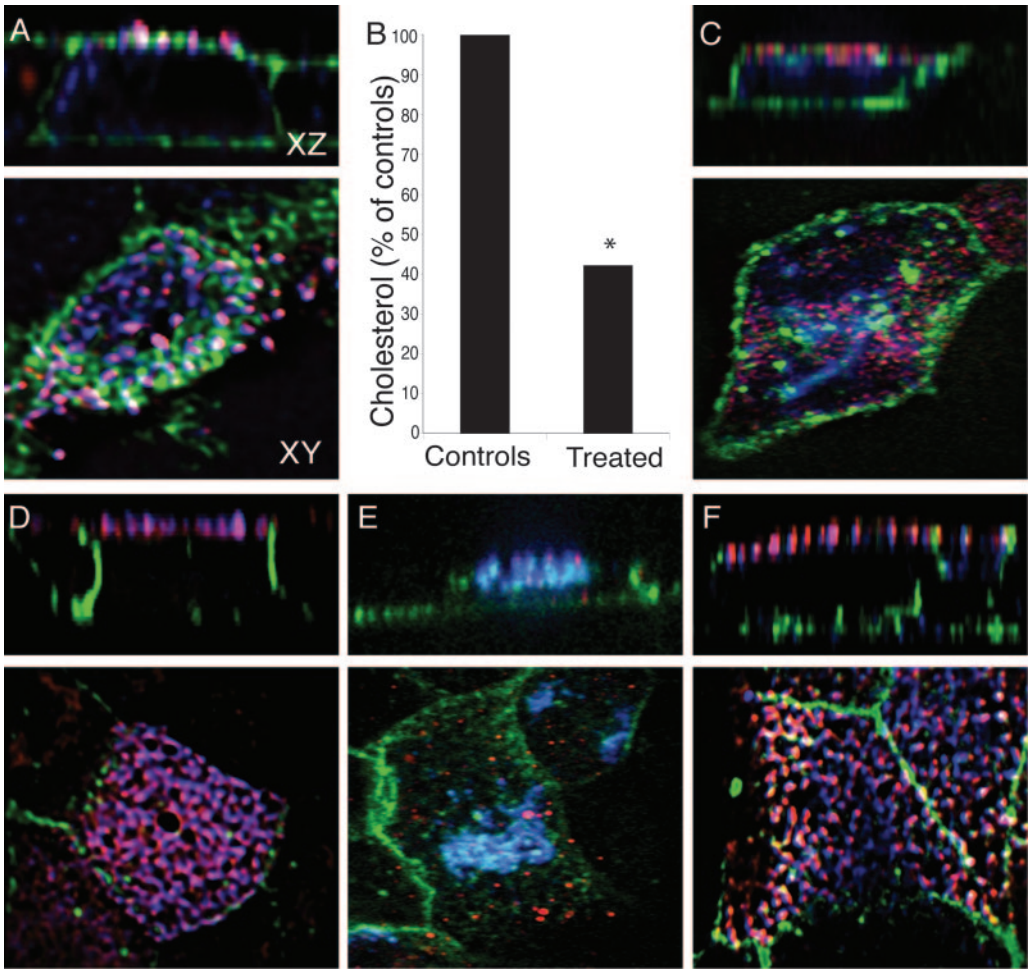

Figure 3. Targeting of CX_3CL1 to the apical membrane of RTEC. (A) MDCK cells that expressed a mutant CX_3CL1 construct that lacks the cytoplasmic tail (MDCK-CX_3CL1–360) were fixed and then incubated with anti-CX_3CL1 Ab and a Cy3-conjugated secondary Ab to visualize cell surface CX_3CL1. For further visualization of intracellular CX_3CL1, the same cells then were permeabilized and then labeled with anti-CX_3CL1 Ab and then Cy5-conjugated secondary Ab. After permeabilization, cells were incubated with Alexa 488–conjugated phalloidin to label F-actin. Slides were examined using a spinning disk confocal microscope. Images are shown as x *versus* y and x *versus* z optical sections. (B) For depletion of cholesterol and disruption of lipid rafts, MDCK-CX_3CL1-GFP cells were incubated for 30 min at 37°C with methyl-β-cyclodextrin (MβCD), and the cholesterol content was measured by spectrophotometry using Amplex Red (Molecular Probes). Values for cholesterol content are expressed as a percentage of untreated controls and represent a mean of three experiments (*$P < 0.05$). (C) MDCK-CX_3CL1-GFP cells were incubated for 30 min with MβCD before fixation and incubation with antibodies as in A. (D) MDCK-CX_3CL1-GFP cells were labeled with anti-CX_3CL1 Ab, as in A, after treatment with benzyl-2-acetamido-2-deoxy-α-D-galacto-pyranoside overnight to inhibit O-glycosylation. (E) MDCK-CX_3CL1-GFP cells were labeled with anti-CX_3CL1 Ab as in A after overnight treatment with tunicamycin to inhibit N-glycosylation. (F) MDCK cells that expressed HA-tagged NHE3 (MDCK-NHE3) were incubated overnight with tunicamycin. The cells then were fixed and incubated with anti-HA Ab and then Cy3-conjugated secondary Ab. For visualization of intracellular NHE3, the same cells were permeabilized and then incubated with anti-HA Ab and then Cy5-conjugated secondary Ab. After permeabilization, the cells also were incubated with Alexa 488–conjugated phalloidin to label F-actin.

fractionated cellular proteins between two distinct fractions—triton soluble and triton insoluble—as described previously (33). In polarized epithelial cells, proteins that were anchored directly to the actin cytoskeleton preferentially remain in the triton-insoluble fraction. We found, however, that CX_3CL1 largely was soluble in triton solution, suggesting that it is not tethered directly to the actin cytoskeleton (Figure 4H). These data also confirm that CX_3CL1 is not associated with lipid rafts (Figures 3C and 4G). Collectively, these data indicate that after sorting to the apical surface, CX_3CL1 is held immobile there, but this is not achieved by direct tethering to the actin cytoskeleton or by association with lipid rafts.

CX_3CL1 Expressed on the Apical Surface of RTEC Promotes Adhesion of Leukocytes

CX_3CL1 can act as a cell adhesion molecule, facilitating the binding of leukocytes (7,43). We therefore hypothesized that CX_3CL1 might perform a similar function when expressed on

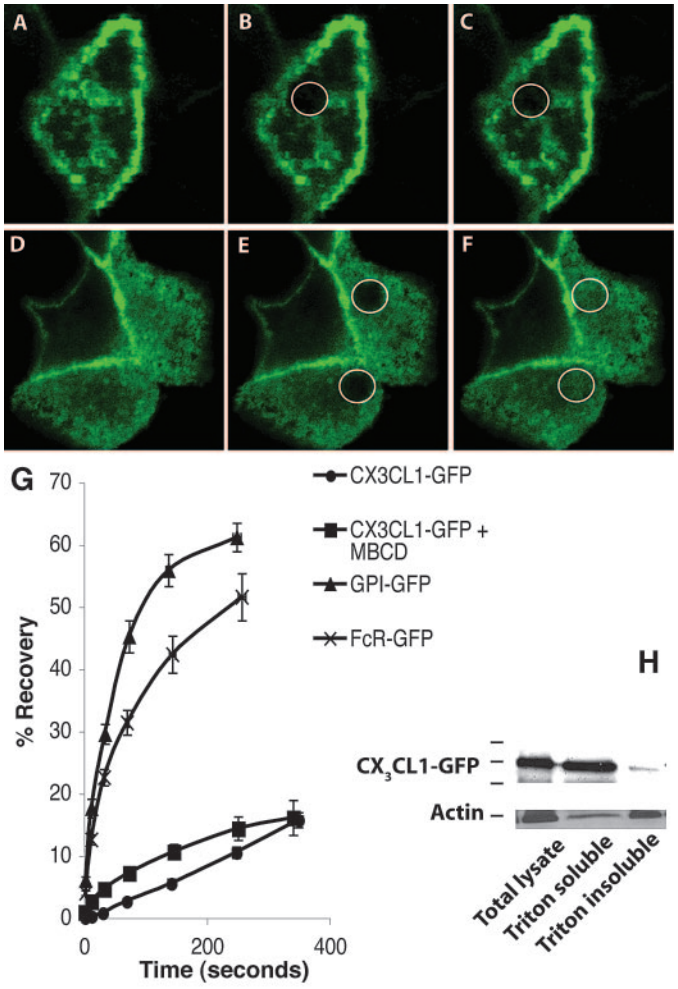

Figure 4. CX_3CL1 is anchored to the apical membrane in RTEC. For examination of the mobility of CX_3CL1 in the apical membrane, fluorescence recovery after photobleaching (FRAP) was performed as described in Materials and Methods. Using an argon laser and a scanning confocal microscope, a 2.5-μM region of the apical membrane that expressed CX_3CL1-GFP was photobleached irreversibly (circles), and recovery of fluorescence was monitored over time. (A) MDCK-CX_3CL1-GFP cell before bleaching. (B) The same cell immediately after photobleaching. (C) The same cell 5 min later. Control areas of the same diameter in the plasma membrane were examined at each time point. (D through F) As a control, FRAP was performed similarly in MDCK cells that expressed freely mobile glycosyl phosphatidylinositol conjugated to GFP (MDCK-GPI-GFP). (D) MDCK-GPI-GFP cells before bleaching. (E) The same cell immediately after bleaching. (F) The same cell after 5 min of recovery. (G) As an additional control, FRAP was performed in MDCK cells that expressed the single transmembrane protein FcγIIa receptor tagged with GFP (FcR-GFP). Recovery of fluorescence after photobleaching of apical CX_3CL1-GFP, GPI-GFP, FcR-GFP, and CX_3CL1-GFP after cholesterol depletion was done with MβCD. Points represent the mean ± SEM of recovery at serial time points from at least six experiments. (H) Lysates from MDCK-CX_3CL1-GFP cells were obtained after separation into triton-soluble and triton-insoluble fractions, as described in Materials and Methods. Western blotting was performed using anti-CX_3CL1 Ab and HRP-conjugated secondary Ab.

the apical surface of RTEC. Under the low-shear conditions used, there was minimal binding of control K562 leukocytes to either MDCK or MDCK-CX_3CL1-GFP cells (data not shown). We found significant binding of K562-CX_3CR1 leukocytes to MDCK-CX_3CL1-GFP cells (Figure 5, A and B). When CX_3CL1 was present on the apical membrane, leukocyte adhesion was almost three times greater than when CX_3CL1 was absent ($P < 0.001$; Figure 5C).

To verify that any observed responses were not an idiosyncratic feature of transformed cell lines, we performed the same experiments using primary, untransfected cells. Human PBMC

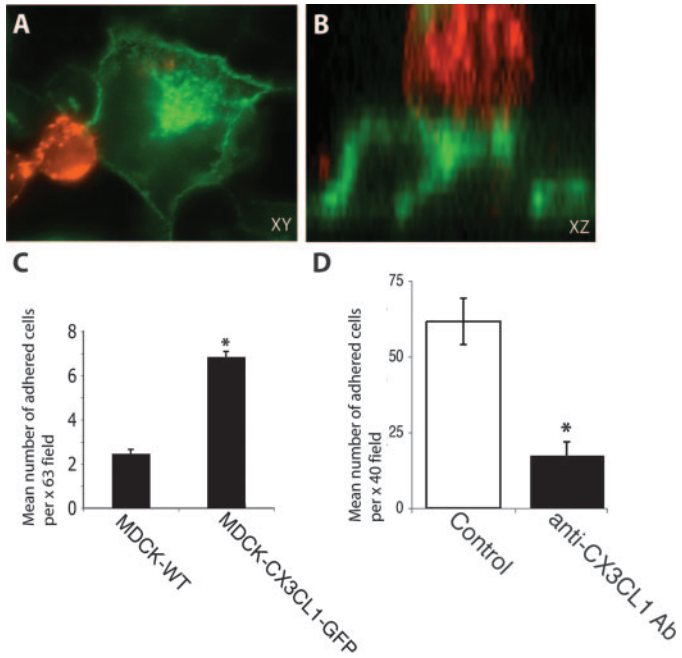

Figure 5. CX_3CR1-expressing leukocytes adhere to CX_3CL1 in the apical membrane of RTEC. K562 cells that expressed the CX_3CR1 receptor (K562-CX_3CR1) were labeled with rhodamine-conjugated cholera toxin B to visualize them. K562-CX_3CR1 cells (1×10^6) were added to MDCK or MDCK-CX_3CL1-GFP monolayers, growing on 25-mm cover slips, under conditions of low-shear stress. After 20 min, nonadherent cells were removed by washing, and the remaining cells were fixed. Serial fields (×63) were examined, using a Leica deconvolution microscope, and the number of adherent cells were counted. (A and B) Photomicrographs of labeled K562-CX_3CR1 cells (red) binding to MDCK-CX_3CL1-GFP monolayers. Images shown in x *versus* y (A) and x *versus* z (B) optical sections. (C) Graph depicting the number of K562-CX_3CR1 leukocytes bound to either MDCK or MDCK-CX_3CL1-GFP cells. Values represent the mean number of adherent cells per high-power field (×63). Values represent the mean of three experiments ± SEM (*$P < 0.001$). (D) Adhesion assays were repeated using primary RTEC and human peripheral blood mononuclear cells (PBMC) that were isolated from the blood of healthy volunteers. In parallel experiments, primary RTEC monolayers were preincubated with function-blocking anti-CX_3CL1 Ab (1 μg/ml) for 30 min before addition of PBMC. Values represent the mean number of adherent PBMC per ×40 field. Experiments were performed six times for each condition (*$P < 0.0001$ *versus* control).

were isolated from heparinized blood of healthy volunteers. PBMC contain multiple leukocyte subsets, including $CD8^+$ T lymphocytes, monocytes, and NK cells, all of which express the CX_3CR1 receptor. PBMC efficiently adhered to the apical surface of monolayers of primary human RTEC. When primary RTEC were preincubated with function-blocking anti-CX_3CL1 Ab, binding of PBMC was inhibited significantly (Figure 5D). Collectively, these data suggest that CX_3CL1 expressed on the luminal surface of RTEC promotes adhesion of leukocytes that bear the complementary receptor CX_3CR1. Our results are in keeping with previous reports in which blockade of CX_3CL1/CX_3CR1 impaired binding of THP-1 monocytic cells to primary proximal RTEC (32).

Discussion

The expression and the function of CX_3CL1 in endothelial cells have been well described (6,7,27,43). In the kidney, an important role for CX_3CL1 has been found in diseases that involve glomerular inflammation and endothelial injury (19,20,22,23). CX_3CL1 also is upregulated in renal tubulointerstitial inflammation, most notably in acute allograft rejection (19), but the specific localization of the chemokine (apical *versus* basolateral) has been somewhat unclear (32). The purpose of these studies, therefore, was to ascertain the subcellular distribution and targeting of CX_3CL1 in polarized tubular epithelial cells. Unexpectedly, we found that transmembrane CX_3CL1 was expressed predominantly on the apical surface of RTEC. This pattern of expression mirrors that found in epithelial cells of biliary ductules (44) but differs markedly from that of intestinal epithelial cells, where CX_3CL1 largely is expressed in the basolateral membrane and in regions of intercellular contact (45,46). In the intestine, as in the kidney, expression of CX_3CL1 is highly enhanced in disease states that are marked by active inflammation (14,45,47).

We next examined how CX_3CL1 is sorted to the apical membrane. In polarized cells, several signals can sort transmembrane proteins to either the basolateral or the apical membrane. The sorting determinant may lie in the cytoplasmic, transmembrane, or extracellular domain of the protein. Sorting signals in the cytoplasmic tail include PDZ domains and dileucine motifs, used by the cystic fibrosis transmembrane regulator and the IgG Fc receptor, respectively (36,37). By deleting the cytoplasmic tail of CX_3CL1, we excluded an apical targeting signal in this region. Other transmembrane proteins, such as Thy-1, apically target through direct or indirect associations with lipid rafts (48). However, when we disrupted any potential association with rafts by extracting cholesterol, we found no change in the distribution of CX_3CL1.

Carbohydrate modification of the protein backbone also may direct trafficking of transmembrane proteins, as is the case for sucrase isomaltase, which requires O-glycosylation for apical targeting (38). CX_3CL1 has 26 O-glycosylation sites in the mucin stalk. However, when we inhibited O-glycosylation, CX_3CL1 still trafficked to the apical membrane. For other proteins, such as endolyn and the glycine transporter GLYT2, N-glycosylation is the crucial determinant of apical targeting (49,50). CX_3CL1 has a single N-glycosylation site, located in the chemokine domain (2). Our studies indicate that glycosylation of this site is the key signal that directs CX_3CL1 to the apical membrane.

We postulated that after translocating to the apical membrane, CX_3CL1 would become anchored there, positioning it to act as a cellular adhesion molecule (7,10,43,51). Firm anchoring of the chemokine within the membrane would allow it to tether passing cells that express the receptor CX_3CR1. Our experiments indicate that CX_3CL1 indeed is immobile, similar to another adhesion molecule, CD44 (42,52).

We next considered how CX_3CL1 might be physically anchored to the apical membrane. Some adhesion molecules, including CD44, are tethered to the cell membrane by direct association with lipid rafts. We therefore examined the effect of cholesterol depletion and disruption of rafts on apical tethering of CX_3CL1. Disruption of lipid rafts did not increase the lateral mobility of CX_3CL1. Moreover, CX_3CL1 segregated with the detergent-soluble, rather than -insoluble, cellular fraction, further refuting a direct association with lipid rafts. These data also suggest that CX_3CL1 is not anchored directly to the actin cytoskeleton. A recent model of membrane fluidity proposed that transmembrane proteins might be fenced into discrete regions of the membrane (53). Such a mechanism might account for the limited lateral mobility of CX_3CL1. Alternatively, CX_3CL1 could be anchored indirectly to the actin cytoskeleton by one or more triton-soluble adaptor proteins (54).

Although our studies demonstrate that CX_3CL1 is targeted and anchored within the apical membrane, the key question is what role it might play there. CX_3CL1 in intestinal epithelium has been shown to recruit leukocytes in inflammation and to regulate cell survival and wound repair (7,45,55). In intestinal epithelium, CX_3CL1 is expressed predominantly on the basolateral surface, where it is in direct contact with CX_3CR1-expressing host leukocytes, including macrophages, lymphocytes, and dendritic cells. In the lamina propria, basolateral CX_3CL1 tethers dendritic cells to intestinal epithelium. Adherent dendritic cells then form transepithelial protrusions, which they extend into the gut lumen, facilitating immunosurveillance and defense against enteroinvasive bacteria (46). In contrast, no such immunosurveillance is known to occur within the kidney or the intrahepatic biliary tree. In biliary ductular epithelial cells, CX_3CL1 is expressed both apically and basolaterally (44,47). CX_3CL1 on the apical surface of regenerating biliary epithelial cells has been implicated in repair of the biliary tree after acute injury, presumably by recruiting hepatic stem cells, which express CX_3CR1 (47). In RTEC, a similar role has been proposed for CD44. CD44 normally is expressed on the basolateral membrane, where it participates in cell–matrix interactions. However, after renal tubulointerstitial injury, CD44 is expressed apically, where it is thought to promote regeneration and repair (56,57).

Conclusion

We have found that CX_3CL1 on the apical membrane promotes tethering of leukocytes that bear the complementary receptor. During tubulointerstitial renal inflammation, tight junctions break down, potentially allowing leukocytes to es-

cape into the urinary space. We postulate that apical CX_3CL1 facilitates recruitment and retention of these leukocytes, redirecting them to the site of injury. In this manner, CX_3CL1 may play an important role in tubulointerstitial nephritis, pyelonephritis, and renal allograft rejection, disease processes in which expression of CX_3CL1 is highly upregulated. As with biliary epithelial cells, CX_3CL1 also may participate in regeneration of tubules after inflammatory injury. Further work is needed to ascertain the *in vivo* functions of CX_3CL1 located on the apical membrane of RTEC.

Acknowledgments

A.M.D. was supported through a studentship through the Hospital for Sick Children Research Training Centre. R.T.A. was supported by the Canadian Child Health Clinician Scientist Program.

We thank Bob Temkin and Michael Ho for technical assistance. We are grateful to Drs. Sergio Grinstein and Andrew Herzenberg for reagents and helpful discussions.

Disclosures

None.

References

1. Moser B, Wolf M, Walz A, Loetscher P: Chemokines: Multiple levels of leukocyte migration control. *Trends Immunol* 25: 75–84, 2004
2. Bazan JF, Bacon KB, Hardiman G, Wang W, Soo K, Rossi D, Greaves DR, Zlotnick A, Schall TJ: A new class of membrane-bound chemokine with a CX3C motif. *Nature* 385: 640–644, 1997
3. Garton KJ, Gough PJ, Blobel CP, Murphy G, Greaves DR, Dempsey PJ, Raines EW: Tumor necrosis factor-alpha-converting enzyme (ADAM17) mediates the cleavage and shedding of fractalkine (CX3CL1). *J Biol Chem* 276: 37993–38001, 2001
4. Hundhausen C, Misztela D, Berkhout TA, Broadway N, Saftig P, Reiss K, Hartmann D, Fahrenholz F, Postina R, Matthews V, Kallen K-J, Rose-John S, Ludwig A: The disintegrin-like metalloproteinase ADAM-10 is involved in constitutive cleavage of CX3CL1 (fractalkine) and regulates CX3CL1-mediated cell-cell adhesion. *Blood* 102: 1186–1195, 2003
5. Tsou C-L, Haskell CA, Charo IF: Tumor necrosis factor-alpha-converting enzyme mediates the inducible cleavage of fractalkine. *J Biol Chem* 276: 44622–44626, 2001
6. Imai T, Hieshima K, Haskell C, Baba M, Nagira M, Nishimura M, Kakizaki M, Takagi S, Nomiyama H, Schall TJ, Yoshie O: Identification and molecular characterization of fractalkine receptor, CX3CR1, which mediates both leukocyte migration and adhesion. *Cell* 91: 521–530, 1997
7. Fong AM, Robinson LA, Steeber DA, Tedder TF, Yoshie O, Imai T, Patel DD: Fractalkine and CX3CR1 mediate a novel mechanism of leukocyte capture, firm adhesion, and activation under physiologic flow. *J Exp Med* 188: 1413–1419, 1998
8. Cybulsky MI, Hegele RA: The fractalkine receptor CX3CR1 is a key mediator of atherogenesis. *J Clin Invest* 111: 1118–1120, 2003
9. Eriksson EE: Mechanisms of leukocyte recruitment to atherosclerotic lesions: Future prospects. *Curr Opin Lipidol* 15: 553–558, 2004
10. Robinson LA, Nataraj C, Thomas DW, Howell DN, Griffiths R, Bautch V, Patel DD, Feng L, Coffman TM: A role for fractalkine and its receptor (CX3CR1) in cardiac allograft rejection. *J Immunol* 165: 6067–6072, 2000
11. Robinson LA, Nataraj C, Thomas DW, Cosby JM, Griffiths R, Bautch V, Patel DD, Coffman TM: The chemokine CX3CL1 regulates NK cell activity in vivo. *Cell Immunol* 225: 122–130, 2003
12. Schafer A, Schulz C, Eigenthaler M, Fraccarollo D, Kobsar A, Gawaz M, Ertl G, Walter U, Bauersachs J: Novel role of the membrane-bound chemokine fractalkine in platelet activation and adhesion. *Blood* 103: 407–412, 2004
13. Umehara H, Bloom E, Okazaki T, Domae N, Imai T: Fractalkine and vascular injury. *Trends Immunol* 22: 602–607, 2001
14. Brand S, Hofbauer K, Dambacher J, Schnitzler F, Staudinger T, Pfennig S, Seiderer T, Tillack C, Konrad A, Goke B, Ochsenkuhn T, Lohse P: Increased expression of the chemokine fractalkine in Crohn's disease and association of the fractalkine receptor T280M polymorphism with a fibrostenosing disease phenotype. *Am J Gastroenterol* 101: 99–106, 2006
15. Rimaniol AC, Till SJ, Garcia G, Capel F, Godot V, Balabanian K, Durand-Gasselin I, Varga E, Simonneau G, Emilie D, Durham SR, Humbert M: The CX3C chemokine fractalkine in allergic asthma and rhinitis. *J Allergy Clin Immunol* 112: 1139–1146, 2003
16. Schwaeble WJ, Stover CM, Schall TJ, Dairaghi DJ, Trinder PK, Linington C, Iglesias A, Schubart A, Lynch NJ, Weihe E, Schafer MK: Neuronal expression of fractalkine in the presence and absence of inflammation. *FEBS Lett* 439: 203–207, 1998
17. Wong BW, Wong D, McManus BM: Characterization of fractalkine (CX3CL1) and CX3CR1 in human coronary arteries with native atherosclerosis, diabetes mellitus, and transplant vascular disease. *Cardiovasc Pathol* 11: 332–338, 2002
18. Chen YM, Lin SL, Chen CW, Chiang W, Tsai TJ, Hsieh BW: Tumor necrosis factor-alpha stimulates fractalkine production by mesangial cells and regulates monocyte transmigration: Down-regulation by cAMP. *Kidney Int* 63: 474–486, 2003
19. Cockwell P, Chakravorty SJ, Girdlestone J, Savage CO: Fractalkine expression in human renal inflammation. *J Pathol* 196: 85–90, 2002
20. Furuichi K, Wada T, Iwata Y, Sakai N, Yoshimoto K, Shimizu M, Kobayashi K, Takasawa K, Kida H, Takeda S, Matsushima K, Yokoyama H: Upregulation of fractalkine in human crescentic glomerulonephritis. *Nephron* 87: 314–320, 2001
21. Inoue A, Hasegawa H, Kohno M, Ito M, Terada M, Imai T, Yoshie O, Nose M, Fujita S: Antagonist of fractalkine (CX3CL1) delays the initiation and ameliorates the progression of lupus nephritis in MRL/lpr mice. *Arthritis Rheum* 52: 1522–1533, 2005
22. Ito Y, Kawachi H, Morioka Y, Nakatsue T, Koike H, Ikezumi Y, Oyanagi A, Natori Y, Nakamura T, Gejyo F, Shimizu F: Fractalkine expression and the recruitment of CX3CR1+ cells in the prolonged mesangial proliferative glomerulonephritis. *Kidney Int* 61: 2044–2057, 2002

23. Feng L, Chen S, Garcia GE, Xia Y, Siani M, Botti P, Wilson CB, Harrison JK, Bacon KB: Prevention of crescentic glomerulonephritis by immunoneutralization of the fractalkine receptor CX3CR1. *Kidney Int* 56: 612–620, 1999
24. Donadelli R, Zanchi C, Morigi M, Buelli S, Batani C, Tomasoni S, Corna D, Rottoli D, Benigni A, Abbate M, Remuzzi G, Zoja C: Protein overload induces fractalkine upregulation in proximal tubular cells through nuclear factor kappaB- and p38 mitogen-activated protein kinase-dependent pathways. *J Am Soc Nephrol* 14: 2436–2446, 2003
25. Pietrzyk MC, Banas B, Wolf K, Rummele P, Woenckhaus M, Hoffman U, Kramer BK, Fischereder M: Quantitative gene expression analysis of fractalkine using laser microdissection in biopsies from kidney allografts with acute rejection. *Transplant Proc* 36: 2659–2661, 2004
26. Reich H, Tritchler D, Herzenberg AM, Kassiri Z, Zhou X, Gao W, Scholey JW: Albumin activates ERK via EGF receptor in human renal epithelial cells. *J Am Soc Nephrol* 16: 1266–1278, 2005
27. Liu GY, Kulasingam V, Alexander RT, Touret N, Fong AM, Patel DD, Robinson LA: Recycling of the membrane-anchored chemokine, CX3CL1. *J Biol Chem* 280: 19858–19866, 2005
28. Robinson LA, Tu L, Steeber DA, Preis O, Platt JL, Tedder TF: The role of adhesion molecules in human leukocyte attachment to porcine vascular endothelium: Implications for xenotransplantation. *J Immunol* 161: 6931–6938, 1998
29. Fong AM, Alam SM, Imai T, Haribabu B, Patel DD: CX3CR1 tyrosine sulfation enhances fractalkine-induced cell adhesion. *J Biol Chem* 277: 19418–19423, 2002
30. D'Souza S, Garcia-Cabado A, Yu F, Teter K, Lukacs G, Skorecki K, Moore HP, Orlowski J, Grinstein S: The epithelial sodium-hydrogen antiporter Na+/H+ exchanger 3 accumulates and is functional in recycling endosomes. *J Biol Chem* 173: 2035–2043, 1998
31. Kurashima K, Szabo EZ, Lukacs G, Orlowski J, Grinstein S: Endosomal recycling of the Na+/H+ exchanger NHE3 isoform is regulated by the phosphatidylinositol 3-kinase pathway. *J Biol Chem* 273: 20828–20836, 1998
32. Chakravorty SJ, Cockwell PP, Girdlestone J, Brooks CJ, Savage CO: Fractalkine expression on human renal tubular epithelial cells: Potential role in mononuclear cell adhesion. *Clin Exp Immunol* 129: 150–159, 2002
33. Hayashi H, Szaszi K, Grinstein S: Multiple modes of regulation of Na+/H+ exchangers. *Ann N Y Acad Sci* 976: 248–258, 2002
34. Alexander RT, Furuya W, Orlowski J, Grinstein S: Rho GTPases dictate the mobility of the Na/H exchanger NHE3 in epithelia: Role in apical retention and targeting. *Proc Natl Acad Sci U S A* 102: 12253–12258, 2005
35. Lippincott-Schwartz J, Presley JF, Zaal KJ, Hirschberg K, Miller CD, Ellenberg J: Monitoring the dynamics and mobility of membrane proteins tagged with green fluorescent protein. *Methods Cell Biol* 58: 261–281, 1999
36. Matter K, Yamamoto EM, Mellman I: Structural requirements and sequence motifs for polarized sorting and endocytosis of LDL and Fc receptors in MDCK cells. *J Cell Biol* 126: 991–1004, 1994
37. Ostedgaard LS, Randak C, Rokhlina T, Karp P, Vermeer D, Ashbourne Excoffon KJ, Welsh MJ: Effects of C-terminal deletions on cystic fibrosis transmembrane conductance regulator function in cystic fibrosis airway epithelia. *Proc Natl Acad Sci U S A* 100: 1937–1942, 2003
38. Naim HY, Joberty G, Alfalah M, Jacob R: Temporal association of the N- and O-linked glycosylation events and their implication in the polarized sorting of intestinal brush border sucrase-isomaltose, aminopeptidase N, and dipeptidyl peptidase IV. *J Biol Chem* 274: 17961–17967, 1999
39. Lisanti MP, Sargiacomo M, Graeve L, Saltiel AR, Rodriguez-Boulan E: Polarized apical distribution of glycosylphosphatidylinositol-anchored proteins in a renal tubular epithelial cell line. *Proc Natl Acad Sci U S A* 85: 9557–9561, 1988
40. Ilangumaran S, Hoessli DC: Effects of cholesterol depletion by cyclodextrin on the sphingolipid microdomains of the plasma membrane. *Biochem J* 335: 433–440, 1998
41. Amundson DM, Zhou M: Fluorometric method for the enzymatic determination of cholesterol. *J Biochem Biophys Methods* 38: 43–52, 1999
42. Oliferenko S, Paiha K, Harder T, Gerke V, Schwarzler C, Schwarz H, Beug H, Gunthert U, Huber LA: Analysis of CD44-containing lipid rafts: Recruitment of annexin II and stabilization by the actin cytoskeleton. *J Cell Biol* 146: 843–854, 1999
43. Goda S, Imai T, Yoshie O, Yoneda O, Inoue H, Nagano Y, Okazaki T, Imai H, Bloom ET, Domae N, Umehara H: CX3C-chemokine, fractalkine-enhanced adhesion of THP-1 cells to endothelial cells through integrin-dependent and -independent mechanisms. *J Immunol* 164: 4313–4320, 2000
44. Isse K, Harada K, Zen Y, Kamihara T, Shimoda S, Harada M, Nakanuma Y: Fractalkine and CX3CR1 are involved in the recruitment of intraepithelial lymphocytes of intrahepatic bile ducts. *Hepatology* 41: 506–516, 2005
45. Muehlhoefer A, Saubermann LJ, Gu X, Luedtke-Heckenkamp K, Xavier R, Blumberg RS, Podolsky DK, MacDermott RP, Reinecker HC: Fractalkine is an epithelial and endothelial cell-derived chemoattractant for intraepithelial lymphocytes in the small intestinal mucosa. *J Immunol* 164: 3368–3376, 2000
46. Niess JH, Brand S, Gu X, Landsman L, Jung S, McCormick BA, Vyas JM, Boes M, Ploegh HL, Fox JG, Littman DR, Reinecker HC: CX3CR1-mediated dendritic cell access to the intestinal lumen and bacterial clearance. *Science* 307: 254–258, 2005
47. Efsen E, Grappone C, DeFranco RM, Milani S, Romanelli RG, Bonacchi A, Caliguri A, Failli P, Annunziato F, Pagliai G, Pinzani M, Laffi G, Gentilini P, Marra F: Up-regulated expression of fractalkine and its receptor CX3CR1 during liver injury in humans. *J Hepatol* 37: 39–47, 2002
48. Powell SK, Lisanti MP, Rodriguez-Boulan EJ: Thy-1 expresses two signals for apical localization in epithelial cells. *Am J Physiol* 260: C715–C720, 1991
49. Potter BA, Ihrke G, Bruns JR, Weixel KM, Weisz OA: Specific N-glycans direct apical delivery of transmembrane, but not soluble or glycosylphosphatidylinositol-anchored forms of endolyn in Madin-Darby canine kidney cells. *Mol Biol Cell* 15: 1407–1416, 2004
50. Martinez-Maza R, Poyatos I, Lopez-Corcuera B, Nu E, Gimenez C, Zafra F, Aragon C: The role of N-glycosylation in transport to the plasma membrane and sorting of the neuronal glycine transporter GLYT2. *J Biol Chem* 276: 2168–2173, 2001
51. Kerfoot SM, Lord SE, Bell RB, Gill V, Robbins SM, Kubes P:

Human fractalkine mediates leukocyte adhesion but not capture under physiological shear conditions; a mechanism for selective monocyte recruitment. *Eur J Immunol* 33: 729–739, 2003
52. Constantin G, Majeed M, Giagulli C, Piccio L, Kim JY, Butcher EC, Laudanna C: Chemokines trigger immediate beta2 integrin affinity and mobility changes: Differential regulation and roles in lymphocyte arrest under flow. *Immunity* 13: 759–769, 2000
53. Suzuki K, Ritchie K, Kajikawa E, Fujiwara T, Kusumi A: Rapid hop diffusion of a G-protein-coupled receptor in the plasma membrane as revealed by single-molecule techniques. *Biophys J* 88: 3659–3680, 2005
54. Neame SJ, Uff CR, Sheikh H, Wheatley SC, Isacke CM: CD44 exhibits a cell type dependent interaction with triton X-100 insoluble, lipid rich, plasma membrane domains. *J Cell Science* 108: 3127–3135, 1995
55. Brand S, Sakaguchi T, Gu X, Colgan SP, Reinecker HC: Fractalkine-mediated signals regulate cell-survival and immune-modulatory responses in intestinal epithelial cells. *Gastroenterology* 122: 166–177, 2002
56. Asselman M, Verhulst A, Van Ballegooijen ES, Bangma CH, Verkoelen CF, De Broe ME: Hyaluronan is apically secreted and expressed by proliferating or regenerating renal tubular cells. *Kidney Int* 68: 71–83, 2005
57. Xie Y, Nishi S, Fukase S, Nakamura H, Chen X, Imai N, Sakatsume M, Saito A, Ueno M, Narita I, Yamamoto T, Gejyo F: Different type and localization of CD44 on surface membrane of regenerative renal tubular epithelial cells in vivo. *Am J Nephrol* 24: 188–197, 2004